

# Modelling of mixed-phase MAPbI<sub>3</sub>

E. Nonni<sup>†</sup>, D. Rossi<sup>†</sup>, M. Auf der Maur<sup>†,\*</sup>, A. Di Carlo<sup>†,‡</sup>

<sup>†</sup>Dept. of Electronic Engineering, Università degli Studi di Roma “Tor Vergata”, Italy

<sup>‡</sup>CNR-ISM, Via Fosso del Cavaliere 100, 00133 Rome, Italy

\*Email: auf.der.maur@ing.uniroma2.it

**Abstract**—Both x-ray diffraction (XRD) and photoluminescence (PL) characterizations of methylammonium lead iodide perovskite (MAPbI<sub>3</sub>) reveal signatures of a coexistence of the tetragonal and orthorhombic phases over a wide range of temperatures, suggesting that the phase transition does not happen sharply at a temperature of 164 K as reported in literature. To understand the causes of this discrepancy we investigated the evolution of the phase mixture from 300 K down to 80 K and its influence on electrical device characteristics. For this we developed a numerical approach to extract effective electrical parameters like resistivity for the mixed-phase MAPbI<sub>3</sub> as a function of temperature and volume ratio of the two phases. The spatial distribution of the tetragonal and orthorhombic phases and their evolution with temperature has been extracted from measured XRD maps, employing a Monte Carlo algorithm to interpolate between measured temperatures. The electrical simulations have been performed by means of the drift-diffusion model.

## I. INTRODUCTION

Despite being one of the most widely used materials in optoelectronics and photovoltaic applications, methyl-ammonium lead iodide (MAPbI<sub>3</sub>, MA = CH<sub>3</sub>NH<sub>3</sub>) physical properties are still under active investigation.

In this work we examine the changes of electrical properties in MAPbI<sub>3</sub> during the tetragonal/orthorhombic phase transition by using a theoretical approach, focusing our analysis on a temperature range of  $80 < T < 300$  K.

According to experimental results observed in temperature dependent resistivity measurements, photo-luminescence (PL) spectroscopy and X-ray diffraction (XRD) [1], [2], the phase transition occurs gradually and exhibits a hysteresis between heating and cooling cycles. By device simulations employing the drift-diffusion model (DD) [3] we investigated the electrical device behavior across this phase transition, based on the experimentally determined phase maps and suitably parameterized mobility and defect state models.

Our study elucidates how the hysteresis affects the resistivity behaviour of MAPbI<sub>3</sub> when cooling or heating the samples with different speed rates. In fact, a wider or narrower hysteresis leads to different resistivity results, highlighting how charge transport measurements can be used to characterize the phase transition.

## II. MODEL AND DISCUSSION

In order to perform transport simulations on realistic phase-mixed structures, we developed an algorithm to generate phase maps that reproduce the characteristics of measured XRD images at given temperatures.

First of all, the experimental XRD image, representing the structure of the two phases of MAPbI<sub>3</sub> at a given temperature, is processed by means of a threshold function. This allows to obtain a binarized image, where each of the two colour shades in the original image is converted into black or white, according to the phase they represent. We used black and white to represent the orthorhombic (OP) and tetragonal (TP) phases, respectively, as shown in an example in Fig. 1. In order to smooth the interfaces a Gaussian smoothing function is also applied. The binarized image is then converted into a matrix where the white pixels are coded with a +1 and the black pixels with a -1. Subsequently, an algorithm that recognizes the boundaries of the white regions is applied. After this step, a list of lines connecting two adjacent points is generated, and whenever a line is closed, a surface is generated. If a surface is completely enclosed in another one a parent-child dependency is detected, allowing the recognition of holes.

The algorithm also detects and deletes double lines and isolated points. In fact, if a surface is too small it will be drawn as a single point or by two superimposed lines. To obtain a complete map, a rectangle with the same dimensions of the original image is created and the black regions are located by subtracting the white ones to the rectangle, always considering the parent-child dependencies for hole detection.

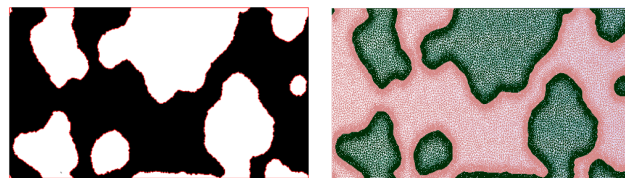


Fig. 1. Binarized image obtained applying a threshold function to the real XRD image (left). The white and black regions identifies the TP and OP respectively, while the red lines trace the edges of white regions. Meshed device used in simulations (right).

Since the availability of real XRD maps is limited to only few temperatures, we developed another algorithm based on the Metropolis Monte Carlo method, exploiting the Ising model [4] to generate artificial maps at any temperature.

Relying on statistical mechanics that defines the probability of a spin to be in one configuration or another (in this case a +1 or -1), and starting with a known configuration of the phases distribution (a real XRD map), the domains expand following an energy minimization principle [5].

If a single spin  $\sigma_m$  flips orientation, the total energy would change by an amount of

$$\Delta E = E_f - E_i = 2J \cdot \sigma_m \sum_n \sigma_n. \quad (1)$$

Here,  $E_f$  and  $E_i$  are the energies after and before the spin flip, respectively.  $J$  is the coupling energy and  $n$  runs over the nearest neighbors of  $m$ .

If  $\Delta E < 0$ , the the spin flips and the associated pixel changes its colour. Otherwise, it will change its spin with a probability proportional to  $\exp(-\Delta E/k_B T)$ , where  $k_B$  is the Boltzmann constant and  $T$  the temperature.

The number of pixels to flip is set interpolating the real tetragonal phase percentages between the discrete temperatures of the measured maps, shown in Fig. 2. The total amount of black and white pixels of a seed image is calculated, and then the algorithm flips the amount of pixels necessary to achieve the percentage of TP at the chosen temperature.

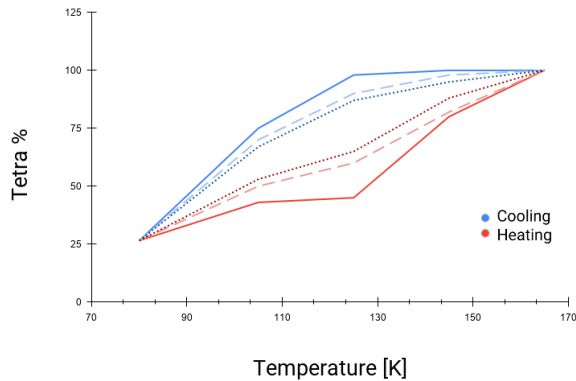


Fig. 2. Tetragonal phase percentage as a function of the temperature for cooling and heating cycles. Interpolating between the two cycles allows to adjust the hysteresis in order to simulate different cooling and heating speed rates, as indicated by the different dashed lines. A narrower hysteresis refers to a slower temperature cycle.

Changing the interpolation function allows a tuning of the hysteretic behaviour of the device, making the cooling/heating rate simulations straightforward.

Simulations were performed exploiting the drift-diffusion model, including trap-assisted (Shockley-Read-Hall) and direct recombination, adding ohmic contacts on the left and right of the mixed-phase structures.

The two perovskite phases have been characterized by specific electrical parameters, namely band parameters, dopant energy level, permittivity and mobility.

Band edges have been set taking into account the different energy gaps of phases leading to the discontinuity detected at TP/OP boundaries, where the corresponding band-offset due to the phase transition is energetically distributed between the conduction and valence band as 75% and 25%, respectively. The band-offset considered in device simulations is obtained from tight-binding bulk calculations [6].

For the mobility we used a standard low field model with a power-law temperature dependence given by [7]

$$\mu = \mu_0 \cdot \left(\frac{T}{T_0}\right)^{-\gamma}, \quad (2)$$

where  $\mu_0$  refers to the mobility at room temperature ( $T_0 = 300$  K) for the two phases and  $\gamma$  is the temperature coefficient.

Fig. 3 shows as an example the effective resistivity as a function of temperature of the mixed-phase perovskite for the cooling and heating cycles, for an applied potential of 5 V. It can be observed that the resistivity exhibits a maximum during the phase transition.

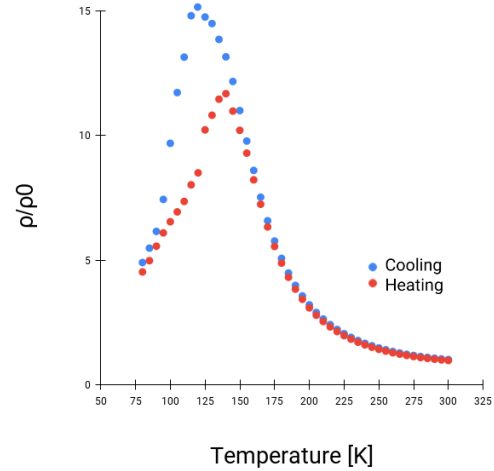


Fig. 3. Resistivity behaviour as a function of temperature for an applied potential 5 V, for the cooling and heating phase, calculated on the generated mixed-phase maps.

## REFERENCES

- [1] A. Osheroov, E. M. Hutter, K. Galkowski, R. Brenes, D. K. Maude, R. J. Nicholas, P. Plochocka, V. Bulović, T. J. Savenije, and S. D. Stranks, “The impact of phase retention on the structural and optoelectronic properties of metal halide perovskites,” *Advanced Materials*, vol. 28, no. 48, pp. 10757–10763, oct 2016.
- [2] V. Campanari, M. Lucci, L. A. Castriotta, B. Paci, A. Generosi, M. Guaragno, R. Francini, M. Cirillo, and A. D. Carlo, “Metal-semiconductor transition in thin film MAPbI3 perovskite,” *Applied Physics Letters*, vol. 117, no. 26, p. 261901, dec 2020.
- [3] M. Auf der Maur, G. Penazzi, G. Romano, F. Sacconi, A. Pecchia, and A. Di Carlo, “The multiscale paradigm in electronic device simulation,” *IEEE Transactions on Electron Devices*, vol. 58, no. 5, pp. 1425–1432, 2011.
- [4] M. P. Team, “Ising model and metropolis algorithm,” *MATLAB Central File Exchange*, (<https://www.mathworks.com/matlabcentral/fileexchange/62194-ising-model-and-metropolis-algorithm>), 2021.
- [5] J. Kotze, “Introduction to monte carlo methods for an ising model of a ferromagnet,” *arXiv preprint arXiv:0803.0217*, 2008.
- [6] A. Di Vito, A. Pecchia, M. Auf der Maur, and A. Di Carlo, “Non-linear work function tuning of lead-halide perovskites by mxenes with mixed terminations,” *Advanced Functional Materials*, vol. 30, no. 47, p. 1909028, 2020.
- [7] A. Biewald, N. Giesbrecht, T. Bein, P. Docampo, A. Hartschuh, and R. Ciesielski, “Temperature-dependent ambipolar charge carrier mobility in large-crystal hybrid halide perovskite thin films,” *ACS Applied Materials & Interfaces*, vol. 11, no. 23, pp. 20838–20844, may 2019.